

Modeling and Experimental Examination of the Solonitsyn Memory Effect on the Surface of Wide Band Gap Metal Oxides[§]

S. A. Polikhova,[†] N. S. Andreev,[†] A. V. Emeline,[‡] V. K. Ryabchuk,[†] and N. Serpone^{*,‡,⊥}

Department of Photonics, Institute of Physics, St. Petersburg State University, St. Petersburg, Russia,
Department of Chemistry & Biochemistry, Concordia University, 7141 Sherbrooke Street West,
Montreal, Quebec, Canada H4B-1R6, and Dipartimento di Chimica Organica, Università di Pavia,
Via Taramelli 10, 27100 Pavia, Italy

Received: August 21, 2003; In Final Form: November 10, 2003

When the surface of a solid semiconductor or dielectric metal oxide (or other) specimen is preirradiated, the solid often retains its photochemical activity after termination of irradiation through formation of long-lived surface-active adsorption centers. This effect has two origins, viz., the so-called Kugel'sberg memory effect and the Solonitsyn memory effect. The former denotes preirradiation in the presence of the adsorbate molecules, whereas the latter refers to preirradiation in vacuo followed by subsequent introduction of adsorbate molecules into the reactor. This article reports results of detailed studies on the Solonitsyn memory effect in gas/solid heterogeneous systems with respect to photostimulated adsorption (i.e. reductive or oxidative adsorption) of molecular oxygen, molecular hydrogen, and methane on the surface of a dielectric metal oxide such as zirconia. The memory effect has been quantified for several metal oxides and alkali halides by means of an experimentally determined postadsorption memory coefficient, $\eta(t)$, which defines the fraction of long-lived photoadsorption centers with respect to the total number of both long-lived and short-lived surface centers of photoadsorption generated for a time of irradiation, t . A simple model is proposed to explain the experimental data.

Introduction

The preirradiated surface of a solid photocatalyst often retains, albeit partly, its photoinduced chemical activity.¹ This effect is described as a memory effect with regard to surface photochemical processes. Adsorption of gas molecules on a photoexcited solid surface represents a simple example of a surface photochemical reaction. The memory effect is observed as postadsorption of gas molecules on the preirradiated surface, the prefix "post" reflecting the situation when adsorption occurs after irradiation of the surface is terminated. There are two different manifestations of the memory effect:² (i) the Kugel'sberg memory effect and (ii) the Solonitsyn memory effect.³ The former is observed as a residual chemical activity of the preirradiated surface in the presence of the adsorbate molecules, whereas the latter effect manifests itself as a conservation of photoinduced surface activity after preirradiation of the sample (typically in vacuo) in the absence of adsorbate molecules.

Photostimulated adsorption is a complex multistep process (typically chemisorption) described as a stoichiometric reaction between adsorbate molecules and the solid surface driven by light absorbed either by the adsorbate or by the solid adsorbent.^{1,4} Often, the process is considered a chemical step (primary) in a photocatalytic reaction. Characteristically, photoadsorption begins from electronic photoexcitation of the solid adsorbent, which leads to generation of free charge carriers (electrons and holes) followed by their migration toward the surface, and subsequent trapping by surface defects (i.e. surface adsorption

centers). The process converts the defects into an active state of the solid in terms of the ability to form chemical bonds with adsorbate molecules.^{1,5} The final step of photoadsorption is the chemical interaction of adsorbate molecules with surface centers in the active state.

An essential feature of a surface-photogenerated adsorption center is that its active state can decay through different physical pathways. Consequently, the active state of the photoinduced adsorption center can be characterized by its lifetime, τ .^{1,6,7} The lower limit of τ can be estimated from the Langmuir–Hinshelwood (LH)-like dependence of the initial (quasi-stationary) rate of photoadsorption on the pressure (p ; concentration) of the adsorbate molecules (eq 1)

$$\left. \frac{dp}{dt} \right|_{t \rightarrow 0} = \frac{k_{\text{exc}} \rho S_0 k_{\text{ad}} p}{k_{\text{dec}} + k_{\text{ad}} p} \quad (1)$$

where $(dp/dt)|_{t \rightarrow 0}$ is the initial rate of photoadsorption; k_{exc} is an apparent rate constant of photoexcitation of surface centers, which converts the centers into their active state; ρ is the photon flow of the incident light; S_0 is the initial concentration of the surface centers of photostimulated adsorption; p is the concentration (pressure) of adsorbate molecules; k_{ad} is the rate constant of adsorption (interaction of adsorbate molecules with surface centers in the active state); and k_{dec} is the apparent pseudo-first-order rate constant of decay of the active state of the surface centers through physical pathways, with $k_{\text{dec}} = 1/\tau$. Typical estimates of the lifetime of the active state of adsorption centers obtained from eq 1 yield lifetimes in the range 1 to 10^{-5} s.^{4,6–9} At the same time, results of experimental studies of post-adsorption effects indicate that the lifetime of a photoinduced active state of adsorption centers can be as much as 10^5 s, and perhaps even longer.^{4,7–12} In the latter case, the lower limit of

* Address correspondence to this author. Fax: (+1) 514-848-2868. E-mail: serpone@vax2.concordia.ca.

[§] Dedicated to the memory of Yu. P. Solonitsyn.

[†] St. Petersburg State University.

[‡] Concordia University.

[⊥] Università di Pavia.

the lifetime of the active state corresponds to the time period between the end of irradiation of the specimen's surface in vacuo and introduction of the adsorbate molecules into the reactor. For technical reasons, the lower limit of the lifetime cannot be less than 1–10 s. Consequently, this value is usually taken as a limit to distinguish between short-lived and long-lived surface active centers. The latter centers are also the specific centers of postadsorption responsible for the Solonitsyn memory effect.

The postadsorption effect has been established for a large number of different heterogeneous systems that includes metal oxides, alkali earth metal fluorides, alkali metal halides, and simple gases (O₂, H₂, CH₄, CO, CO₂, and some others) with the lifetime of the active state of photoinduced long-lived adsorption centers typically longer than 10⁴ s.^{4,7–12}

One of the quantitative parameters that characterizes the memory effect is the postadsorption memory coefficient,^{1,4} η , defined by eq 2,

$$\eta(t) = \frac{N_{ps}(t)}{N_{ph}(t)} = \frac{\Delta p_{ps}(t)}{\Delta p_{ph}(t)} \quad (2)$$

where $N_{ps}(t)$ is the total number of molecules postadsorbed on the (photo)adsorbent surface after the latter is preirradiated in vacuo for a time t , and is directly proportional to the change of pressure $\Delta p_{ps}(t)$ in a closed reactor during postadsorption. Note that $N_{ps}(t)$ is directly proportional to the number of long-lived adsorption centers that conserved their active state after irradiation stopped (in the simplest case of monomolecular adsorption $N_{ps}(t)$ equals the number of such long-lived centers). The relationship $N_{ph}(t) \propto \Delta p_{ph}(t)$ represents the total number of molecules photoadsorbed for the same time period t during irradiation of the specimen's surface in the presence of adsorbate molecules. The latter term must be and typically has been measured at sufficiently high pressure to fulfill the condition $k_{ad}p \gg k_{dec}$ (eq 1), which is required to make all the physical pathways for decay of the active state negligible relative to the pathway responsible for adsorption. In this case, the rate of photoadsorption is proportional to the rate of photogeneration of the active state of surface adsorption centers. Thus, the term $N_{ph}(t)$ is proportional (or is equal to, in the case of monomolecular adsorption) to the number of adsorption centers converted into the active state for the time t of irradiation. Consequently, the postadsorption memory coefficient shows the fraction of long-lived (photo)adsorption centers with respect to the total number of both long-lived and short-lived surface centers of photoadsorption generated during the time of irradiation.

The experimental data for the postadsorption memory coefficient measured for some heterogeneous gas/solid heterogeneous systems are summarized in Table 1. For most of the heterogeneous systems examined at long times of irradiation ($t > 10$ min), the postadsorption memory coefficient usually lies in the range 0.05 to 0.15. A significant exception was observed only in the case of ZnO.¹³ To explain that $\eta < 1$, a simple assumption was made of the coexistence (co-generation) of two different types (long-lived and short-lived) of adsorption centers. It is relevant to emphasize that the memory coefficient depends strongly on the time of irradiation. For short times of irradiation (e.g., $t < 1$ min; see Table 1), η is greater than for longer times of irradiation. This infers that at short irradiation times the fraction of long-lived adsorption centers is significantly large. However, the experimental dependence (eq 1) that establishes the lifetime (typically in the millisecond range) of short-lived adsorption centers is observed from the initial rate of photo-

TABLE 1: Experimental Values of Postadsorption Memory Coefficients Determined at Short ($t \leq 1$ min) and Long ($t \geq 10$ min) Times of Irradiation for Different Photoadsorbents^a

photo- adsorbent	refs	adsorbate					
		O ₂		H ₂		CH ₄	
		$t^b > 10$	$t^b < 1$	$t^b > 10$	$t^b < 1$	$t^b > 10$	$t^b < 1$
ZnO	11, 24	0.65	0.9	—	—	0.45	0.52
BeO	11, 24	0.1	0.5	0.52	0.75	0.47	0.60
MgO	11, 24	0.12	0.42	—	—	—	0.35
γ -Al ₂ O ₃	11, 24	0.17	0.57	—	—	—	—
MgAl ₂ O ₄ ^c	9	0.12	—	0.09	—	—	—
Sc ₂ O ₃ ^c	8	0.05	—	—	—	—	—
Ga ₂ O ₃	11, 24	0.17	0.6	—	—	—	—
SiO ₂	11, 24	0.25	0.58	0.3	—	0.3	—
GeO ₂	11, 24	0.12	0.22	0.07	0.12	0.1	—
ZrO ₂ ^c	15	0.14	—	—	—	—	—
KBr ^c	23	0.05	—	no photoadsorption			
NaF	23	0.25	—	—	—	—	—
RbI	23	0.15	—	no photoadsorption			

^a Where no values are given, the memory coefficient was not measured. ^b t in minutes. ^c Systems for which the dependence of the initial rate of photoadsorption on the pressure of the gases indicated was examined.

adsorption. At very short times of irradiation, $\eta \rightarrow 1$ (see, for example, refs 6–9). At the same time, for the long-lived adsorption centers with lifetimes of the active state around 10⁴ s, the condition that $k_{ad}p \gg k_{dec}$ is already fulfilled at very low pressures of the adsorbate molecules (range 10^{−6}–10^{−5} Pa). Consequently, at low pressures one should observe an apparent independence of the photoadsorption rate on pressure p (eq 1). However, this is not observed in the experimental dependencies, at least for some of the heterogeneous systems identified in Table 1. Apparently, the considered experimental data appear to be in contradiction with the assumption of the coexistence (co-generation) of two different (long-lived and short-lived) types of adsorption centers commonly used to explain the physical sense of the memory coefficient.

In the present article, we report relevant results of detailed studies of the Solonitsyn memory effect in gas/solid heterogeneous systems with respect to photostimulated adsorption of molecular oxygen, molecular hydrogen, and methane on the surface of the dielectric material zirconia. We also provide a simple model to explain the experimental data.

Experimental Section

The powdered monoclinic ZrO₂ specimen was of high purity grade (“7–4”, IREA, Russia) having a specific surface area of ca. 7 m² g^{−1} (BET method; nitrogen gas). The specimen was pretreated in a manner identical with that described earlier^{7,14} to remove ubiquitous organic impurities and any other adventitious adsorbed molecules. Reproduction of the original state of the specimens between experiments was achieved by heating the samples at 800 K in an oxygen atmosphere for about 1 h. Experimental errors in the measurements caused by the non-reproducibility of the original state of the specimen are unlikely to exceed ca. $\pm 10\%$.

The powdered specimen (ca. 500 mg) was contained in a quartz cell (path length 3 mm; illuminated area 6 cm²) connected to a high-vacuum setup equipped with an oil-free pump system. The residual gas pressure in the reaction cell was ca. 10^{−7} Pa, measured with a Pirani-type manometer (sensitivity: 18 mV Pa^{−1} for O₂, 24 mV Pa^{−1} for H₂, and 28 mV Pa^{−1} for CH₄). The chemical composition of the gas phase, the partial pressure of the gases, and the nature of desorption products were

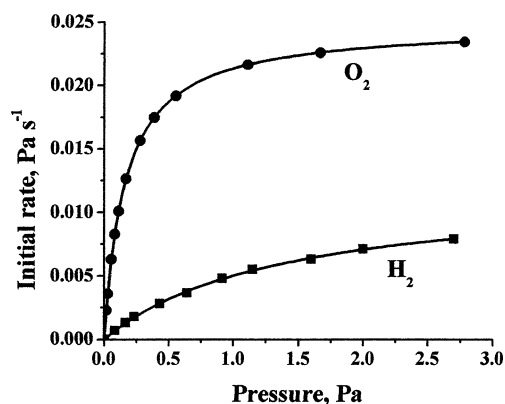


Figure 1. Dependencies of the initial rates of photostimulated adsorption of oxygen and hydrogen on zirconia as a function of gas pressure.

monitored with a mass spectrometer (model MX7301) connected to the reactor.

Irradiation of the solid specimens was achieved with a 120-W high-pressure mercury lamp {MELZ, DRK-120; photon flow at wavelengths less than 260 nm was ca. 2×10^{14} photons cm⁻² s⁻¹}. Metal-supported neutral quartz filters (Vavilov SOI) were used to vary the intensity of the actinic light.

A thermoprogrammed device (TPD) was used to record the thermodesorption spectra of photoadsorbed and postadsorbed gases on the surface of ZrO₂. The working temperature range of the device was 300–800 K with the rate of linear temperature increase set at 0.3 K s⁻¹.

Experimental Results

Figure 1 shows the dependencies of the initial rates of photoadsorption of molecular oxygen and molecular hydrogen on the gas pressure. Both dependencies follow the typical LH-type kinetics described by eq 1. In further experiments, all measurements relevant to the photostimulated adsorption and post adsorption of gases on zirconia were made at pressures corresponding to the independence of the initial rates with respect to the gas pressure. Note that although the dependence of the initial rate of photoadsorption of methane on pressure was not obtained, in control experiments we demonstrated that the initial rate remained constant at methane pressures greater than 3 Pa used in further experiments.

The relevant kinetic data for the evolution of $\Delta p_{ph}(t)$ and $\Delta p_{ps}(t)$, which are directly proportional to the number of photoadsorbed and postadsorbed molecules of selected gases (oxygen, hydrogen, and methane), respectively, as a function of the time of irradiation, are summarized in Figure 2, panels a, b, and c. In addition, the temporal accumulation of photoadsorbed and postadsorbed molecules of oxygen was also monitored by TPD measurements at each time of irradiation. The corresponding thermoprogrammed desorption spectra of molecular oxygen are illustrated in Figure 3, panels a and b, respectively. We note that both photoadsorbed and postadsorbed oxygen desorbed in three (presumably) different forms at 400, 500, and 600 K. From the shape of the TPD spectra for oxygen, it is obvious that at short times of irradiation (curve 1) the contribution of the oxygen species desorbed at 400 K is slightly greater than that for the two other forms.

In earlier studies,^{7,14,15} we inferred that centers of oxygen postadsorption are the surface electron defects, namely surface Zr³⁺ ions, and the F⁺ and F centers on the basis of diffuse reflectance spectra. Electron paramagnetic resonance methods (EPR) identified the adsorbed form of oxygen in the case of

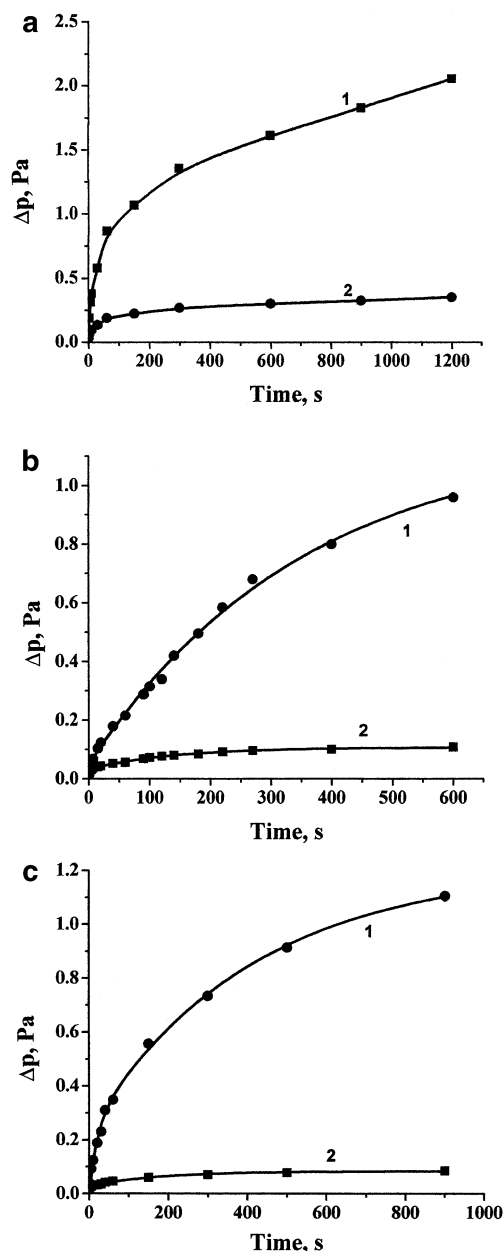


Figure 2. (a) Temporal dependencies of the accumulation of photoadsorbed (1) and postadsorbed (2) oxygen on the zirconia particle surface. [Note: these manometric data are, within experimental error, in complete accord with the TPD data (not shown); see, for example, Figure 5]. (b) Temporal dependencies of the accumulation of photoadsorbed (1) and postadsorbed (2) hydrogen on the zirconia particle surface. (c) Temporal dependencies of the accumulation of photoadsorbed (1) and postadsorbed (2) methane on the zirconia particle surface.

both photoadsorption and postadsorption as the superoxide radical anion O₂^{•-} ($g_1 = 2.0312$, $g_2 = 2.099$, $g_3 = 2.0040$).¹⁶ Accordingly, we conclude that there exist several forms of adsorbed oxygen on ZrO₂ that differ only by the type of adsorption centers as is typical of wide band gap (photo)adsorbents.⁴ Therefore, it is appropriate to estimate a partial memory coefficient for each form of adsorbed molecules to compare them with predictions from the proposed model (see below). Since the population of all three forms increases with increasing irradiation time, more or less proportionately, estimates of the memory coefficient using the total number of photoadsorbed and postadsorbed molecules are close to the correct coefficient for each form of the adsorbed oxygen molecules. Similar

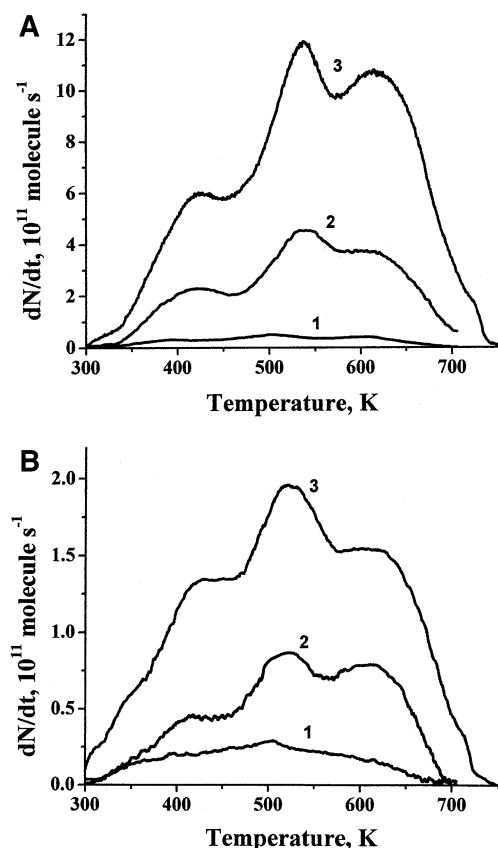


Figure 3. (a) Temperature-programmed desorption (TPD) spectra of photoadsorbed oxygen at different times of irradiation: (1) 5, (2) 30, and (3) 300 s. (b) Temperature-programmed desorption spectra of postadsorbed oxygen at different times of irradiation: (1) 5, (2) 30, and (3) 300 s.

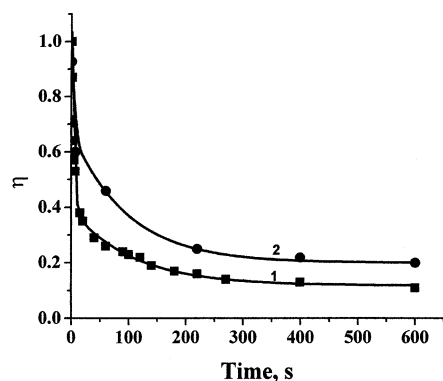


Figure 4. Dependences of the memory coefficient of hydrogen postadsorption on the zirconia particle on the time of irradiation: (1) irradiation in vacuo and (2) irradiation in the presence of oxygen.

assumptions were made for adsorption of molecular hydrogen and methane. Unfortunately, it was not possible to determine the forms of adsorbed molecules in the latter two cases by TPD methodology, since increased temperature caused desorption of the product of the dissociative adsorption of the two donor gases (H_2O , CO_2 , C_2H_6 , and others), rather than the original adsorbate molecules as was the case for oxygen.

Experimental dependences of the postadsorption memory coefficients on irradiation time for adsorption of molecular hydrogen, and oxygen and methane on the zirconia particle surface are presented in Figures 4 and 5, respectively. The memory coefficient for oxygen was determined by employing both the manometric and TPD methodologies. The experimental data for all heterogeneous systems investigated show that the

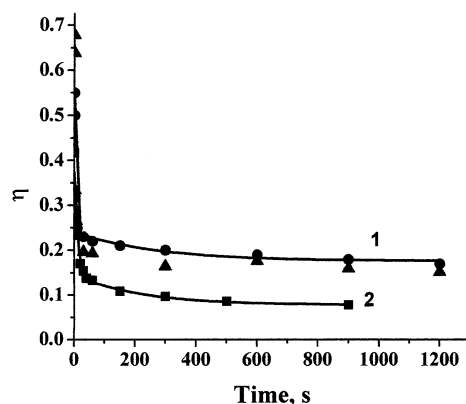


Figure 5. Dependences of the memory coefficient for oxygen (1) {●} memory coefficient measured by the manometric method and (▲) memory coefficient determined from TPD spectra} and for methane (2) postadsorption on the zirconia particle surface on the time of irradiation.

memory coefficients decreased with increasing irradiation time. At the longer irradiation times, the coefficients tended toward a constant value of 0.15, whereas at shorter irradiation times the memory coefficients approached unity. Note that postadsorption of hydrogen on zirconia preirradiated in vacuo is also accompanied by a photoinduced chesoluminescence (PhICL) emission.^{17,18}

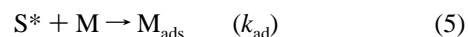
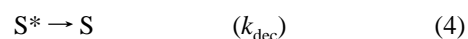
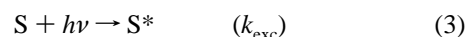
The dependence of the postadsorption memory coefficient determined for the case of postadsorbed hydrogen, with preirradiation of zirconia carried out in the presence of oxygen (also caused photoadsorption of oxygen), is illustrated in Figure 4. As is evident from curve 2, the limit of the memory coefficient at longer times of irradiation is distinctively greater than is otherwise the case for preirradiation in vacuo.

By changing the time of delay between the termination of irradiation of the surface in vacuo and introduction of the gas into the reactor to measure N_{ps} in the interval 1 to 3×10^3 s, the independence of the memory coefficient was demonstrated for several different times of irradiation, t . Consequently, the lifetime of the active state of the surface centers of postadsorption is greater than 3×10^3 s. The recognition of the interchangeability law for the memory coefficient with regard to light intensity and time of irradiation was also demonstrated. The memory coefficient, which is a function of photon flow and irradiation time {i.e. $\eta = f(n, t)$ }, remained constant within experimental error when the light intensity decreased 2-, 5-, and 14-fold with a corresponding increase of the time of irradiation to maintain the product term ρt constant. This interchangeability was ascertained to be valid for both N_{ps} and N_{ph} terms in eq 2.

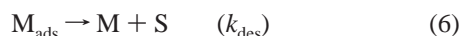
Discussion

The Model. To start the discussion of the experimental results, we first consider the simple model of photoadsorption employed by Rapoport and co-workers⁶ to rationalize the dependence of the initial rate of photoadsorption on the concentration (pressure) of adsorbate molecules. The model is summarized by reactions 3–5 (Mechanism I),

Mechanism I



where the first stage (reaction 3) represents the process of photoexcitation of the photoadsorbent leading to formation of the active state (S^*) of the adsorption center (S). The second stage (reaction 4) depicts the deactivation of the active state through physical pathways, whereas the third stage (reaction 5) describes the adsorption interaction of the adsorbate molecule (M) with the active state of the surface center to form the adsorption complex (M_{ads}). The set of kinetic equations corresponding to this three-stage mechanism of adsorption yields eq 1, which permits determination of the lifetime of the active state of the adsorption centers, $\tau = 1/k_{\text{dec}}$ (see Introduction). Addition of a fourth stage (reaction 6) to describe the decay of the



adsorption complexes through a desorption process restores the surface center to its original state, typical of most metal oxide photoadsorbents. This last stage can be referred to either as a thermodesorption or a photodesorption of photoadsorbed molecules. According to this simple mechanism, the number of surface centers in the active state photogenerated in vacuo at the time of irradiation, t , is determined by reactions 3 and 4. Applying the quasi-steady-state approach for the concentration of surface centers (S_0) in the active state yields expression 7.

$$S^*_t = \frac{k_{\text{exc}}}{k_{\text{exc}} + k_{\text{dec}}} S_0 (1 - e^{-(k_{\text{exc}} + k_{\text{dec}})t}) \quad (7)$$

At sufficiently high pressures, when the physical pathways of deactivation of surface active centers are negligible compared to the adsorption pathway (i.e., $k_{\text{adp}} \gg k_{\text{dec}}$) and the rate of photoadsorption is equal to the rate of photogeneration of surface active centers, the concentration of the photoadsorbed molecules M_{ads} is then given by eq 8. Assuming that $N_{\text{ps}}(t) = S^*_t$ and $N_{\text{ph}}(t) = M_{\text{ads}} t$, the memory coefficient for the adsorption of a molecule

$$M_{\text{ads}} t = \frac{k_{\text{exc}}}{k_{\text{exc}} + k_{\text{des}}} S_0 (1 - e^{-(k_{\text{exc}} + k_{\text{des}})t}) \quad (8)$$

on a given type of adsorption center at the time of irradiation t is given by eq 9

$$\eta(t) = \frac{k_{\text{exc}} + k_{\text{des}}}{k_{\text{exc}} + k_{\text{dec}}} \times \frac{(1 - e^{-(k_{\text{exc}} + k_{\text{dec}})t})}{(1 - e^{-(k_{\text{exc}} + k_{\text{des}})t})} = \eta_{\infty} \frac{(1 - e^{-(k_{\text{exc}} + k_{\text{dec}})t})}{(1 - e^{-(k_{\text{exc}} + k_{\text{des}})t})} = \eta_{\infty} \frac{(1 - e^{-(k_{\text{exc}} + k_{\text{des}}/\eta_{\infty})t})}{(1 - e^{-(k_{\text{exc}} + k_{\text{des}})t})} \quad (9)$$

where η_{∞} is the postadsorption memory coefficient at infinite time of irradiation $t \rightarrow \infty$ (eq 10).

$$\eta_{\infty} = \eta(t)|_{t \rightarrow \infty} = \frac{k_{\text{exc}} + k_{\text{des}}}{k_{\text{exc}} + k_{\text{dec}}} \quad (10)$$

It is evident from eq 9 that at the short times of irradiation, that is as $t \rightarrow 0$, then $\eta(t \rightarrow 0) \rightarrow 1$ under any conditions. Therefore, for a given type of adsorption center and a given form of adsorbed molecules, the dependence of the memory coefficient on the time of irradiation begins from unity at $t \rightarrow 0$ and approaches a limit η_{∞} at $t \rightarrow \infty$, which is determined by the relationship between k_{des} and k_{dec} . According to eq 10, when $k_{\text{des}} > k_{\text{dec}}$, that is when the efficiency of desorption of (photo)-adsorbed molecules is greater than the efficiency of physical decay of the active state of adsorption centers $\eta_{\infty} > 1$ and the memory coefficient increases with increasing time of irradiation,

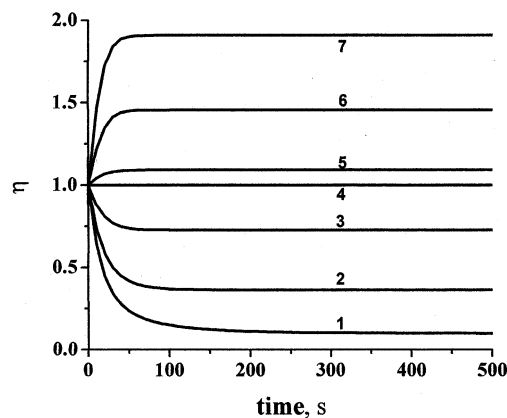


Figure 6. Model dependencies of the memory coefficient on irradiation time based on the solution to eq 9 with different ratios of $k_{\text{des}}/k_{\text{dec}}$: (1) 0.01, (2) 0.3, (3) 0.7, (4) 1, (5) 1.1, (6) 1.5, and (7) 2.

whereas when $k_{\text{des}} < k_{\text{dec}}$, that is when the efficiency of desorption of (photo)adsorbed molecules is less than the efficiency of physical decay of the active state of adsorption centers, then $\eta_{\infty} < 1$ and the dependence of the memory coefficient on the irradiation time decreases accordingly. The curvature of the dependence is dictated by the relationship between k_{exc} and k_{des} on one hand and between k_{exc} and k_{dec} on the other. The curvature is significant when k_{exc} is comparable with or is much smaller than k_{des} and k_{dec} , but is very weak when $k_{\text{exc}} \gg k_{\text{des}}$ and $k_{\text{exc}} \gg k_{\text{dec}}$ tending toward unity. The set of corresponding model curves of the memory coefficient as a function of irradiation time is depicted in Figure 6. Note that an increase of the memory coefficient with irradiation time remains yet to be observed experimentally.

In the case where there exist several types of adsorption centers, the memory coefficient follows expression 11

$$\eta(t) = \frac{\sum_i \frac{k_{\text{exc } i}}{k_{\text{exc } i} + k_{\text{dec } i}} S_{0i} (1 - e^{-(k_{\text{exc } i} + k_{\text{dec } i})t})}{\sum_i \frac{k_{\text{exc } i}}{k_{\text{exc } i} + k_{\text{des } i}} S_{0i} (1 - e^{-(k_{\text{exc } i} + k_{\text{des } i})t})} \quad (11)$$

where S_{0i} is the initial concentration of the adsorption centers of the i th-type and $k_{\text{exc } i}$, $k_{\text{dec } i}$, and $k_{\text{des } i}$ are the corresponding rate constants of the steps for the i th-type of adsorption centers or forms of adsorbed molecules.

After irradiation is terminated, the concentration of a given type of adsorption centers for irradiation in vacuo and the concentration of a given type of (photo)adsorbed form of the adsorbate molecules for irradiation in the presence of such adsorbate obey expressions 12 and 13, respectively,

$$S^*(t') = S^*_t e^{-k_{\text{dec}}(t'-t)} \quad (12)$$

$$M_{\text{ads}}(t') = M_{\text{ads } t} e^{-k_{\text{des}}(t'-t)} \quad (13)$$

where $S^*(t')$ and $M_{\text{ads}}(t')$ are the concentrations of the adsorption centers in the active state and of the adsorbed molecules, respectively, at time $t' > t$, where t is the time at which irradiation was terminated. Thus, the memory coefficient changes after terminating irradiation in accordance with eq 14

$$\eta(t') = \frac{S^*_t e^{-k_{\text{dec}}\tau_{\text{del}}}}{M_{\text{ads } t} e^{-k_{\text{des}}\tau_{\text{del}}}} = \eta_t e^{-(k_{\text{dec}} - k_{\text{des}})\tau_{\text{del}}} \quad (14)$$

where $\eta(t')$ is the memory coefficient at time t' , η_t is the memory coefficient determined at the moment t that irradiation is stopped, and $\tau_{\text{del}} = (t' - t)$ is the time between the moment of termination of irradiation, t , and the moment of determination of the memory coefficient t' . In the general case then, the memory coefficient depends on the time of delay of the measurement. From eq 14, when $k_{\text{dec}} > k_{\text{des}}$ the memory coefficient decreases with increasing delay time, whereas when $k_{\text{dec}} < k_{\text{des}}$ it increases with increasing delay time. The memory coefficient remains constant only in two circumstances: (i) when $k_{\text{dec}} = k_{\text{des}}$, a very uncommon case, and (ii) when $k_{\text{dec}} = 0$ and $k_{\text{des}} = 0$, which means that both deactivation and desorption processes in Mechanism I are photoinduced and do not occur in the absence of irradiation.

The Experimental Results. In the most common case, photoexcitation of the electronic subsystem of a solid (photo)-adsorbent in either the *intrinsic* or *extrinsic* absorption bands leads to generation of free charge carriers (electrons, e, and holes, h), and subsequently to formation of photoinduced adsorption centers as a result of trapping of these free charge carriers by the surface defects, S (i.e., intrinsic defects or impurities), reactions 15 and 16. {Note that Mechanism II is comprised of reactions 15 and 16, and reactions 23–28 given below}.

Mechanism II



Stages 15 and 16 correspond to stage 3 in the model Mechanism I described above with the corresponding pseudo-first-order rate constants given by

$$k_{\text{exc}} = \sigma_S u_e [e_s] \quad (17a)$$

$$= k_e [e_s] \quad (17b)$$

and

$$k_{\text{exc}} = \sigma_S u_h [h_s] \quad (18a)$$

$$= k_h [h_s] \quad (18b)$$

where σ_S is the cross-section of either electron or hole trapping by the adsorption center in the corresponding process, u_e and u_h are the velocities of the electrons and holes, respectively, and $[e_s]$ and $[h_s]$ are the surface concentrations of electrons and holes, respectively, that can be determined by using the approach reported earlier by Emeline and co-workers.^{5,19,20}

In the simplified case of a uniform photogeneration of free charge carriers in the bulk of the solid specimen, the concentration of photogenerated carriers is given by

$$[e] = \alpha_e \rho \tau_e \quad (19)$$

$$[h] = \alpha_h \rho \tau_h \quad (20)$$

where α is the absorption coefficient of photoactive light absorption, ρ is the photon flow, and τ_e and τ_h are the corresponding lifetimes of free electrons and holes, respectively. Consequently, the excitation rate constants are given by

$$k_{\text{exc}} = k_e \alpha_e \rho \tau_e \quad (21)$$

$$k_{\text{exc}} = k_h \alpha_h \rho \tau_h \quad (22)$$

The existence of a short-lived active state of the adsorption centers is confirmed by the dependence of the initial rate of photoadsorption on the initial gas pressure in accordance with eq 1 (see Figure 1) with experimental values of the apparent $k_{\text{dec}} (=1/\tau)$ equal to ca. 10^3 s for oxygen adsorption centers and ca. 10^3 for hydrogen adsorption centers under broadband light irradiation. Mechanisms through which the active state of adsorption centers can decay include the following:^{5,7} (i) thermoionization, which is typical for shallow trapped charge



carriers (reactions 23 and 24), (ii) photoionization (reactions 25 and 26), which is rather typical for deep traps with absorption



bands located within the spectral range of photoexcitation (typically in the near-UV and visible range), and (iii) recombination with free charge carriers of the opposite sign (reactions 27 and 28).



In a previous article,⁷ we demonstrated that the lifetime of the active state of adsorption centers on the zirconia particle surface depends on light intensity and on the spectral composition of the actinic light. The process of thermoionization decay is rather insignificant for deep traps. An estimate of the efficiency of the photoionization pathway of deactivation of adsorption centers shows that the impact of photoionization is also somewhat negligible. By contrast, the recombination pathway for decay of the active state of adsorption centers provides very good agreement with experimental results, and appears to correlate with the experimental results. Accordingly, we can assume that the rate constant of decay of the active state of adsorption centers on the zirconia particle surface subjected to irradiation can be described by eqs 29 and 30. That is,

$$k_{\text{dec}} = \sigma_{\text{Sre}} u_e [e_s] \quad (29a)$$

$$= k_{\text{re}} [e_s] \quad (29b)$$

$$= k_{\text{re}} \alpha_e \rho \tau_e \quad (29c)$$

and

$$k_{\text{dec}} = \sigma_{\text{Srh}} u_h [h_s] \quad (30a)$$

$$= k_{\text{rh}} [h_s] \quad (30b)$$

$$= k_{\text{rh}} \alpha_h \rho \tau_h \quad (30c)$$

where σ_{Sre} is the cross-section of electron recombination with a hole trapped by the adsorption center and σ_{Srh} is the cross-section of hole recombination with an electron trapped on the corresponding adsorption center. Both concentrations of adsorption centers responsible for postadsorption and photoadsorption of gaseous molecules on the surface of zirconia do not change after irradiation is terminated, at least within the experimental delay time of up to ca. 3×10^3 s. Thus, we conclude that both $k_{\text{dec}} = 0$ and $k_{\text{des}} = 0$ in the dark, the consequence of which is

the photoinduced deactivation and desorption processes of adsorption centers (when such processes occur). In keeping with these expectations, photodesorption of prephoadsorbed oxygen on zirconia was recently reported by Emeline and co-workers.^{14,21}

The mechanism of photodesorption of oxygen can be described by reaction 31



with the corresponding pseudo-first-order rate constant given by expression 32

$$k_{\text{des}} = \sigma_{\text{des}} u_{\text{h}} [h_{\text{s}}] \quad (32)$$

where σ_{des} is the cross-section of hole trapping by the photoadsorbed molecules of oxygen. No photodesorption of either hydrogen or methane preadsorbed on zirconia was observed. Therefore, we infer that for these two gases also $k_{\text{des}} = 0$ under irradiation. Note that the experimental observation of $k_{\text{dec}} = 0$ after termination of irradiation is completely satisfied by the recombination pathway of decay of the active state of adsorption centers. Indeed, in the dark, that is when $\rho = 0$ in eqs 29 and 30, there are no photogenerated free charge carriers, and consequently there is no recombination with carriers trapped by adsorption centers during irradiation. Accordingly, $k_{\text{dec}} = 0$ in the dark.

Substitution of eqs 17 (18) and 29 (30) into eq 9 yields expression 33 for the dependence of the postadsorption memory coefficient on the time of preirradiation

$$\eta(t) = \frac{\sigma_e \tau_e + \sigma_{\text{des}} \tau_h}{\sigma_e \tau_e + \sigma_{\text{rh}} \tau_h} \times \frac{(1 - e^{-(\sigma_e \tau_e + \sigma_{\text{rh}} \tau_h) \alpha \rho t})}{(1 - e^{-(\sigma_e \tau_e + \sigma_{\text{des}} \tau_h) \alpha \rho t})} = \eta_{\infty} \frac{(1 - e^{-(\sigma_e \tau_e + \sigma_{\text{rh}} \tau_h) \alpha \rho t})}{(1 - e^{-(\sigma_e \tau_e + \sigma_{\text{des}} \tau_h) \alpha \rho t})} \quad (33)$$

where η_{∞} is given by

$$\eta_{\infty} = \eta(t)|_{t \rightarrow \infty} = \frac{\sigma_e \tau_e + \sigma_{\text{des}} \tau_h}{\sigma_e \tau_e + \sigma_{\text{rh}} \tau_h} \quad (34)$$

and $\eta(t \rightarrow 0) \rightarrow 1$ under any conditions in a manner otherwise identical to the general Mechanism I described by stages 3 to 6. Note that η_{∞} does not depend on light intensity (photon flow). It is determined by the cross-sections of trapping of the corresponding carriers by adsorption centers in either the inactive or active states, by adsorbed molecules (see e.g., steps 15, 27, and 31), and by the lifetime of the corresponding charge carriers. Note also that both the numbers of photoadsorbed and postadsorbed molecules and the memory coefficient obey the interchangeability law. That is, all these parameters remain constant if ρt is constant. Therefore, the model of a single type of adsorption center whose active state is formed by charge carrier trapping by the surface defect and decays through recombination with the charge carrier of the opposite sign describes completely the experimental data obtained in the present study of the Solonitsyn memory effect occurring on zirconia particles. Consequently, the memory coefficient in this model represents the fraction of adsorption centers in the active state that escaped recombination decay during photoexcitation in vacuo and, therefore, were able to stay in the active state for an infinite time after termination of irradiation relative to the number of photoinduced adsorption active centers that reacted

with adsorbate molecules to form the adsorption complex, thereby avoiding photodesorption decay.

As noted earlier (Introduction), the most typical centers for photoadsorption and postadsorption of oxygen on zirconia are the surface Zr^{3+} ions, and the F^+ and F centers formed through electron trapping either by low-coordinated surface Zr^{4+} ions or by anion vacancies, V_{a} , respectively. Photoadsorption and postadsorption of hydrogen and methane involve surface V-type hole centers formed as a result of free hole trapping by surface cation vacancies, V_{c} . Therefore, an appropriate description of the memory behavior of the heterogeneous system is given by eq 11 for the multicenter photostimulated adsorption of gases. However, as shown in previous studies,^{14,15} the kinetic behavior of the photoinduced formation of different electron color centers and hole color centers is similar. Hence, we deduce that the cross-sections of charge carrier trapping and recombinations by the corresponding surface defects are also similar. To a first approximation then, we can consider the behavior of the memory coefficient as described by the model for a single type of adsorption center (eq 33). Note that the recombination mechanism of decay of the active state of adsorption centers on the zirconia surface was also demonstrated earlier from studies⁷ of the dependencies of the initial rate on pressure (concentration) at different light intensities and spectral ranges of photoexcitation. On the basis of experimental results, we deduce that the proposed model completely describes the behavior of the memory coefficient of photoinduced adsorption of gases on zirconia, and does not contradict previous experimental results. Consequently, the memory effect for zirconia originates from the photogeneration of adsorption centers whose lifetime is limited by the recombination process during photoexcitation of the sample, and becomes infinite after termination of irradiation.

As predicted by eq 33, the memory coefficient (particularly its value for an infinite time of irradiation, η_{∞}) depends on the lifetime of charge carriers. This corresponds to the experimentally observed increase of the memory coefficient of hydrogen adsorption at infinite times of irradiation, η_{∞} , on zirconia preirradiated in the presence of oxygen (Figure 4). Indeed, the physical pathway for the formation of the active state of hydrogen adsorption centers is the trapping of free holes (reaction 27). As shown in previous studies,^{5,7,8} the lifetime of free holes during photoexcitation in vacuo can be described by eq 35,

$$\tau_{\text{h}} = \frac{1}{\sum_i k_{\text{exc } i} D_i + k_{\text{dec}} S_e} \quad (35)$$

whereas photoexcitation in the presence of hydrogen gives the lifetime of holes defined by eq 36.

$$\tau_{\text{h}} = \frac{1}{\sum_i k_{\text{exc } i} D_i + k_{\text{des}} M_{\text{ads}}} \quad (36)$$

Since the efficiency of photodesorption of oxygen due to hole trapping is much less than the efficiency of recombination decay of the active state of the adsorption center (where S_e denotes the adsorption centers of oxygen in the active state with a trapped electron, and M_{ads} represents the photoadsorbed oxygen), the lifetime of the holes during photoexcitation in oxygen becomes longer. This results in an increase of the photoexcitation rate constant, k_{exc} (eq 21), and so according to eq 7, the number of hydrogen adsorption centers in the active state also

increases. The result of this is an increase of the memory coefficient in accordance with experimental results. This effect is closely connected to the influence of the photoadsorption of the gas on the formation of photoinduced color centers (photo-coloration).^{8,14,15} In fact, the law of charge conservation requires that after irradiation in vacuo, the number of trapped electrons, F , must be equal to the number of trapped holes, V .^{14,15} That is,

$$F = V \quad (37)$$

whereas after irradiation in oxygen the same condition is given by

$$F + O_{2\text{ ads}} = V \quad (38)$$

resulting in an increase in the number of hole centers, in particular surface hole centers for hydrogen adsorption (eq 38 minus eq 37). In turn, increasing the number of surface centers for hydrogen postadsorption causes an increase of the memory

$$\Delta F + O_{2\text{ ads}} = \Delta V \quad (39)$$

coefficient (eq 33). Accordingly, this demonstrates once again that the memory effect is closely connected to the formation of photoinduced defects in solids.

Conclusions

This article has proposed a model for the adsorption center that fully describes the memory effect examined experimentally for the photostimulated adsorption of acceptor and donor gaseous molecules in such heterogeneous systems as O_2/ZrO_2 , H_2/ZrO_2 , and CH_4/ZrO_2 . According to the model, the active state of the adsorption center is formed as a result of charge carrier trapping by surface defects, with the lifetime of the active state limited by the recombination with free charge carrier of the opposite sign during photoexcitation of the solid. Consequently, when irradiation is terminated and free charge carriers no longer exist to recombine with the active state of the adsorption center, its lifetime becomes infinite leading to the observation of the memory effect in terms of photoinduced adsorption or post-adsorption of gases on a preirradiated surface. In other words, adsorption centers of the same type behave as centers with a short-lived active state during photoexcitation, whereas in the dark the adsorption centers turn into centers with a long-lived active state that is responsible for the postadsorption (Solonitsyn memory) effect. Note that the dependencies obtained in the present studies for gas–solid heterogeneous systems involving zirconia are typical of most other gas–solid heterogeneous systems, inferring that the proposed mechanistic model may be a rather general one.

We should also note that to the extent that the photostimulated adsorption relates to photocatalysis, the Solonitsyn memory effect also relates to photoinduced catalytic processes when preirradiation of the catalyst creates new catalytic centers that are active in the dark and require no additional photoexcitation.

A typical example of such processes is the photoinduced isotope exchange reaction.⁴ Another example of a postirradiation (memory) effect in photocatalysis was recently reported for the reductive degradation of 4-chlorophenol in aqueous TiO_2 dispersions in the presence of hole scavengers.²²

Acknowledgment. We thank the Natural Sciences and Engineering Research Council of Canada for support of our studies through a Discovery Grant (No. A-5443 to N.S.). We are also particularly grateful to the North Atlantic Treaty Organization for a Collaborative Linkage Grant [No. PDD(CP)-PST.CLG-979700] between our respective laboratories, as well as with the laboratory of Prof. V. Otroshchenko of the Bakh Institute of Biochemistry, Moscow.

References and Notes

- (1) Emeline, A. V.; Serpone, N. *Int. J. Photoenergy* **2002**, 4, 91.
- (2) Baru, V. G.; Volkenstein, Th. Th. *The effect of irradiation on surface properties of semiconductors*; Nauka: Moscow, USSR, 1978.
- (3) Solonitsyn, Yu. P. *Russ. J. Phys. Chem.* **1958**, 32, 1241.
- (4) Basov, L. L.; Kuzmin, G. N.; Prudnikov, I. M.; Solonitsyn, Yu. P. *Uspekhi Fotoniiki*; Vilesov Th. I., Ed.; Leningrad State University: Leningrad, USSR, 1976; Issue 6, p 82.
- (5) Serpone, N.; Salinaro, A.; Emeline, A. V.; Ryabchuk, V. K. *J. Photochem. Photobiol. A: Chem.* **2000**, 130, 83.
- (6) Rapoport, V. L.; Antipenko, B. M.; Malkin, M. G. *Kinet. Katal.* **1968**, 9, 1306.
- (7) Emeline, A. V.; Rudakova, A. V.; Ryabchuk, V. K.; Serpone, N. *J. Phys. Chem. B* **1998**, 102, 10906.
- (8) Emeline, A. V.; Petrova, S. V.; Ryabchuk, V. K.; Serpone, N. *Chem. Mater.* **1998**, 10, 3484.
- (9) Emeline, A. V.; Ryabchuk, V. K. *Russ. J. Phys. Chem.* **1997**, 71, 1881.
- (10) Ryabchuk, V. K., *Catal. Today* **2000**, 58, 89.
- (11) Yurkin, V. M. Studies of Memory Effect for Photoadsorption of Simple Molecules on Metal Oxides, Ph.D. Thesis, Leningrad State University, 1984.
- (12) Kuznetsov, V. N.; Lisachenko, A. A. *Uspekhi Fotoniiki*; Vilesov Th. I., Ed.; Leningrad State University: Leningrad, USSR; 1980; Issue 7, p 48.
- (13) Derkach, V. I.; Drobinin, A. N.; Prudnikov, I. M.; Solonitsyn, Yu. P. *Kinet. Katal.* **1982**, 23, 718.
- (14) Emeline, A. V.; Kataeva, G. V.; Litke, A. S.; Rudakova, A. V.; Ryabchuk, V. K.; Serpone, N. *Langmuir* **1998**, 14, 5011.
- (15) Ryabchuk, V. K.; Burukina, G. V. *Russ. J. Phys. Chem.* **1991**, 65, 1621.
- (16) Burukina, G. V. Studies of Photostimulated Adsorption Processes and their Connection with Defect Formation in Metal Oxides, Abstract of Ph.D. Thesis, Leningrad State University, 1990.
- (17) Andreev, N. S.; Emeline, A. V.; Khudnev, V. A.; Polikhova, S. A.; Ryabchuk, V. K.; Serpone, N. *Chem. Phys. Lett.* **2000**, 325, 288.
- (18) Emeline, A. V.; Polikhova, S.; Andreev, N. S.; Ryabchuk, V. K.; Serpone, N. *J. Phys. Chem. B* **2002**, 106, 5956.
- (19) Emeline, A. V.; Ryabchuk, V. K.; Serpone, N. *J. Phys. Chem. B* **1999**, 103, 1316.
- (20) Emeline, A. V.; Frolov, A. V.; Ryabchuk, V. K.; Serpone, N. *J. Phys. Chem. B* **2003**, 107, 7109.
- (21) Emeline, A. V.; Khudnev, S. V.; Ryabchuk, V. K. *Vestnik SpbSU*; State University of St. Petersburg: St. Petersburg, Russia, 1999; Issue 4, Vol. 18, p 23.
- (22) Serpone, N.; Textier, I.; Emeline, A. V.; Pichat, P.; Hidaka, H.; Zhao, J. *J. Photochem. Photobiol. A: Chem.* **2000**, 136, 145.
- (23) Ryabchuk, V. K.; Basov, L. L.; Solonitsyn, Yu. P. *Uspekhi Fotoniiki*; Vilesov, Th. I., Ed.; Leningrad State University: Leningrad, USSR, 1980; Issue 7, p 3.
- (24) Solonitsyn, Yu. P.; Prudnikov, Yu. M.; Yurkin, V. M. *Russ. J. Phys. Chem.* **1982**, 57, 2028.